Exact Real-Time Longitudinal Correlation Functions of the Massive *XXZ* Chain

Constantin Babenko,[1] Frank Göhmann,[1] Karol K. Kozlowski,[2] Jesko Sirker,[3] and Junji Suzuki[4]
[1]*Fakultät für Mathematik und Naturwissenschaften, Bergische Universität Wuppertal, 42097 Wuppertal, Germany*
[2]*Univ Lyon, ENS de Lyon, Univ Claude Bernard, CNRS, Laboratoire de Physique, F-69342 Lyon, France*
[3]*Department of Physics and Astronomy, and Manitoba Quantum Institute, University of Manitoba, Winnipeg R3T 2N2, Canada*
[4]*Department of Physics, Faculty of Science, Shizuoka University, Ohya 836, Suruga, Shizuoka, Japan*

(Received 16 December 2020; accepted 23 April 2021; published 25 May 2021)

We apply a recently developed thermal form factor expansion method to evaluate the real-time longitudinal spin-spin correlation functions of the spin-$\frac{1}{2}$ *XXZ* chain in the antiferromagnetically ordered regime at zero temperature. An analytical result incorporating all types of excitations in the model is obtained, without any approximations. This allows for the accurate calculation of the real-time correlations in this strongly interacting quantum system for arbitrary distances and times.

DOI: 10.1103/PhysRevLett.126.210602

Dynamical correlation functions relate experimental observables like structure factors and transport coefficients to the microscopic details of quantum many-body systems. They are notoriously hard to calculate as they simultaneously probe all timescales and length scales. A particular class of many-body systems are integrable one-dimensional (1D) systems with short-range interactions. Because of the existence of a large number of local conserved quantities, they exhibit a peculiar phenomenology: they do not relax to a thermal equilibrium and can possess spin and charge currents which do not fully decay in time. These unusual properties are not only of fundamental interest but can be observed in experiments on systems which are almost integrable. This includes realizations of the 1D Bose gas in which quench dynamics as well as dynamical correlations in equilibrium have been studied [1–5]. The Heisenberg chain can be realized using cold atomic gases in optical lattices giving direct access to the spin dynamics in the spatiotemporal domain and to spin transport phenomena [6–9]. Good realizations of the Heisenberg chain also occur as substructures in solid state systems [10–12]. Here they provide access to response functions in the momentum-frequency domain as, for example, the dynamical spin-structure factor (DSF) [13]. They also allow for the direct measurement of transport coefficients [14–17]. Recent attempts to devise a general description of 1D close-to-integrable systems resulted in interesting phenomenological theories like the nonlinear Luttinger liquid [18–22] or generalized hydrodynamics [23–27]. It is highly desirable to underpin such new phenomenologies with microscopic calculations. We note, moreover, that dynamical correlation functions in cold atomic gases can now be tested at timescales which are beyond the reach of modern numerical techniques. An exact calculation of dynamical correlation functions of 1D integrable models is therefore important for our understanding of state-of-the-art experiments. At the same time, it provides benchmarks for phenomenological theories and numerical methods.

Exact results on correlation functions are rather rare, even in low dimensions, and are mostly related to models belonging to the free fermion (FF) category [28]. For the Ising model in the scaling limit, a remarkable link to the Painlevé equations was established [29]. Dynamical correlations were studied for the XY model [30] and interesting phenomena of thermalization were addressed. An important next step was to go beyond FF and deal exactly with interacting systems. The vertex operator approach (VOA) opened up a new avenue to do so based on form factor expansions [31]. The evaluation of the two- and four-spinon contributions to the transverse DSF of the massive *XXZ* chain [32–34] and of the four-spinon contribution in the *XXX* limit [35] were important outcomes of this method. The complexity of the resultant multiple integrals has, however, hindered any further analysis. A hidden FF structure in the *XXZ* model was unveiled in Refs. [36,37], and its remarkable outcome, the fermionic basis, yields exact correlation functions up to considerably large distances [38,39]. The application of this method, however, has been limited to the static case so far. The quantum inverse scattering method (QISM) provides a complementary approach [40,41], based on a determinant formula for the scalar product of on-shell and off-shell Bethe vectors [42]. Under restrictions on the possible excitations, it successfully reproduces the asymptotic correlation functions [43,44] predicted by conformal field theory (CFT) [45]. Yet, in order to recover the DSF for the full range of frequencies and momenta, bound states must be taken into account, which are neglected in the CFT limit [46].

In this Letter we employ a recently developed [47,48] form factor expansion for real-time correlation functions in equilibrium and obtain a simple, explicit, closed-form expression including all orders of excitations. We consider the XXZ chain with Hamiltonian

$$H = J\sum_{j=1}^{L}\{\sigma_{j-1}^{x}\sigma_{j}^{x} + \sigma_{j-1}^{y}\sigma_{j}^{y} + \Delta\sigma_{j-1}^{z}\sigma_{j}^{z}\} - \frac{h}{2}\sum_{j=1}^{L}\sigma_{j}^{z} \qquad (1)$$

for length $L \to \infty$. Here σ_j^α are Pauli matrices, and $J > 0$ is the exchange constant. We restrict ourselves to the antiferromagnetically ordered regime, characterized by values $\Delta = \cosh(\gamma) > 1$ of the anisotropy and by magnetic fields in the range $0 < h < 4J\sinh(\gamma)\vartheta_4^2(0|q)$. Here we have set $q = \mathrm{e}^{-\gamma}$, and the ϑ_a denote elliptic theta functions [49]. The special functions appearing here and below are summarized in the Supplemental Material [50].

In the antiferromagnetically ordered regime, the one-body properties of the elementary excitations are characterized by

$$p(\theta) = \frac{\pi}{2} + \theta - i\ln\left(\frac{\vartheta_4(\theta + i\gamma/2|q^2)}{\vartheta_4(\theta - i\gamma/2|q^2)}\right), \qquad (2)$$

$$\varepsilon(\theta) = \frac{h}{2} - 2J\sinh(\gamma)\vartheta_3(0|q)\vartheta_4(0|q)\frac{\vartheta_3(\theta|q)}{\vartheta_4(\theta|q)}, \qquad (3)$$

where $p(\theta)$ is the dressed momentum, $\varepsilon(\theta)$ the dressed energy and θ the rapidity of the quasiparticle. The interaction between excitations is described by the soliton scattering matrix,

$$S(\theta) = \mathrm{e}^{i(\frac{\pi}{2}+\theta)}\frac{\Gamma_{q^4}(1+\frac{i\theta}{2\gamma})\Gamma_{q^4}(\frac{1}{2}-\frac{i\theta}{2\gamma})}{\Gamma_{q^4}(1-\frac{i\theta}{2\gamma})\Gamma_{q^4}(\frac{1}{2}+\frac{i\theta}{2\gamma})}, \qquad (4)$$

where Γ_q denotes the q-gamma function. Because of the Yang-Baxter integrability of the model, any multiparticle scattering can be reduced to multiple two-body scattering events. One then naturally expects that correlation functions can be described solely by (2)–(4). We will show that an all-order expansion of the longitudinal dynamical correlation functions can indeed be described by these physical quantities with supplemental special functions of the q-gamma function family.

Our framework combines the QISM and the quantum transfer matrix (QTM) method [54–56]. The latter has been devised for the investigation of finite temperature bulk quantities and static correlation functions [57,58]. It was generalized in Ref. [47], inspired by Ref. [59], to obtain form factor expansions of dynamical correlations at finite temperatures. We thus call it the thermal form factor expansion method. It has been successfully applied to the analysis of a FF model, the XX model [47,60].

Although we are interested in the dynamical correlations in the ground state, we start from finite temperatures and consider the limits $h, T \to 0$. This may look redundant at first, but there are advantages of this approach. It is well known that the diagonalization of the Hamiltonian leads to string excitations of various lengths [61–63]. These are solutions of the Bethe ansatz equations which form regular patterns ("strings") in the complex plane for $L \to \infty$. Some quantities which characterize the correlations become singular if they are evaluated at the ideal string positions, e.g., $S(\pm i\gamma)$. The variety of string excitations and singularities leads to serious technical difficulties. The VOA provides an alternative description, free from string excitations, but its answer suffers from the high intricacy of multiple integrals. On the other hand, the QTM method, based on a mapping of the 1D quantum system to a two-dimensional classical system, does not directly deal with the Hamiltonian but rather with a transfer matrix acting in an auxiliary space. The possible excitations are thus different from those in the Hamiltonian basis. A previous study, using the higher level Bethe ansatz equations, concludes that only simple excitations are possible for $L \to \infty$ and $h, T \to 0$ with the limit $T \to 0$ taken first [64]. Their distribution in the complex rapidity plane can be interpreted as particle-hole excitations. A rapidity y_j of a particle excitation is situated on a curve located above $[-\pi/2;\pi/2]$ such that $\mathrm{Im}y_j \sim (\gamma/2)$, while a hole rapidity x_j is located below and $\mathrm{Im}x_j \sim -(\gamma/2)$. These excitations are *not* 2 strings since $\Re(y_j - x_l)$ is generically nonzero and $\Im(y_j - x_l)$ does *not* approach γ, even for $L \to \infty$. Thus, the QTM excitations do not produce the aforementioned singularities.

For the longitudinal correlation functions

$$\langle\sigma_1^z(t)\sigma_{m+1}^z(0)\rangle = \lim_{T\to 0}\mathrm{tr}\{\sigma_1^z(t)\sigma_{m+1}^z(0)\exp(-H/T)\}/Z,$$

where Z is the partition function, the relevant excited states consist of an equal number of particles and holes. Thus, the resultant form factor expansion involves a sum over ℓ, the number of particles and holes, and a sum over their possible locations. The higher level Bethe ansatz analysis shows that they obey a one-body equation for $T \to 0$. The sum over the possible locations is then replaced by simple integrations [50],

$$\begin{aligned} G(m,t) &:= \langle\sigma_1^z(t)\sigma_{m+1}^z(0)\rangle - (-1)^m\left(\frac{\vartheta_1{}'(0|q)}{\vartheta_2(0|q)}\right)^2 \\ &= \sum_{\substack{\ell\geq 1\\ k=0,1}}\frac{(-1)^{km}}{(\ell!)^2}\int_{C_-}\frac{d^\ell x}{(2\pi)^\ell} \\ &\quad\times\int_{C_+}\frac{d^\ell y}{(2\pi)^\ell}\mathrm{e}^{-i\sum_{j=1}^{\ell}[mp(x_j)-\varepsilon(x_j)t]} \\ &\quad\times e^{i\sum_{j=1}^{\ell}[mp(y_j)-\varepsilon(y_j)t]}\mathcal{A}^{zz}(\{x_i\}_{i=1}^{\ell},\{y_j\}_{j=1}^{\ell}|k) \\ &= \sum_{\ell\geq 1}I_\ell(m,t). \end{aligned} \qquad (5)$$

The integer $k \in \{0,1\}$ labels the degenerate ground states and we have subtracted the contribution of the staggered magnetization. There is some freedom to choose the contours $C_\pm$: the simplest choice is to take straight segments of length π whose imaginary parts are $\pm\gamma/2+\delta$ where δ is positive. We will discuss the optimal choice of the contours for a numerical evaluation later.

The main purpose of the Letter is to present the explicit form of $\mathcal{A}^{zz}$. It consists of determinants of two $\ell\times\ell$ matrices $\mathcal{M}$ and $\widehat{\mathcal{M}}$ and a scalar part. For a compact presentation, we will use the shorthand notations

$$P_j = e^{2iy_j}, \qquad H_j = e^{2ix_j}, \qquad 1\le j\le \ell,$$

and introduce the basic hypergeometric series [49,65],

$$\Phi_1(P_j) = {}_{2\ell}\Phi_{2\ell-1}\left(\begin{matrix} q^{-2}, \{q^2\frac{P_j}{P_i}\}_{i\neq j}, \{\frac{P_j}{H_i}\}_{i=1}^{\ell} \\ \{\frac{P_j}{P_i}\}_{i\neq j}, \{q^2\frac{P_j}{H_i}\}_{i=1}^{\ell}\end{matrix}; q^4, q^4\right),$$

$$\Phi_2(P_j,P_i) = {}_{2\ell}\Phi_{2\ell-1}\left(\begin{matrix} q^6, \{q^6\frac{P_i}{P_r}\}_{r\neq i,j}, q^2\frac{P_i}{P_j}, \{q^4\frac{P_i}{H_r}\}_{r=1}^{\ell} \\ \{q^4\frac{P_i}{P_r}\}_{r\neq i,j}, q^8\frac{P_i}{P_j}, \{q^6\frac{P_i}{H_r}\}_{r=1}^{\ell}\end{matrix}; q^4, q^4\right). \tag{6}$$

They originate from sums of residues of the soliton S matrix at a particular series of poles. We further introduce

$$r_\ell(P_j,P_i) = \frac{q^2(1-q^2)^2\frac{P_i}{P_j}}{(1-\frac{P_i}{P_j})(1-q^4\frac{P_i}{P_j})}\prod_{r=1}^{\ell}\frac{1-\frac{P_i}{H_r}}{1-q^2\frac{P_i}{H_r}}\prod_{r\neq i,j}^{\ell}\frac{1-q^2\frac{P_i}{P_r}}{1-\frac{P_i}{P_r}} \tag{7}$$

and conveniently write $\Psi_2(P_j,P_i) = r_\ell(P_j,P_i)\Phi_2(P_j,P_i)$. The matrix element $\mathcal{M}_{ij}$ is then given by

$$\mathcal{M}_{ij} = \delta_{ij}D_{ij} + (1-\delta_{ij})E_{ij} \tag{8}$$

with

$$D_{ij} = \bar{\Phi}_1(P_j) - \Phi_1(P_j)(-1)^k\prod_{r=1}^{\ell}\frac{S(y_j-y_r)}{S(y_j-x_r)},$$

$$E_{ij} = -\bar{\Psi}_2(P_j,P_i) + \Psi_2(P_j,P_i)(-1)^k\prod_{r=1}^{\ell}\frac{S(y_i-y_r)}{S(y_i-x_r)}. \tag{9}$$

Here we define for any function $g(P_1,\ldots,H_1,\cdots)$,

$$\bar{g}(P_1,\ldots,H_1,\cdots) \coloneqq g(P_1^{-1},\ldots,H_1^{-1},\cdots).$$

The matrix element $\widehat{\mathcal{M}}_{ij}$ is obtained from $\mathcal{M}_{ij}$ by replacing all $y_r\leftrightarrow -x_r$. Then $\mathcal{A}^{zz}$ is explicitly represented as

$$\mathcal{A}^{zz} = \det(\mathcal{M})\det(\widehat{\mathcal{M}})\left(\frac{\mu^\ell\vartheta_1'(0|q)\sin\mathcal{P}}{\vartheta_1(\Sigma|q)}\right)^2 \times\frac{\prod_{1\le i<j\le\ell}\psi_D(x_i-x_j)\psi_D(y_i-y_j)}{\prod_{i,j}\psi_D(x_i-y_j)}. \tag{10}$$

We set $\mathcal{P} = \frac{\pi k}{2} + \sum_l\{[p(y_l)-p(x_l)]/2\}$, $\Sigma = -(\pi k/2)+\sum_l(y_l-x_l)/2$,

$$\psi(\theta) = \Gamma_{q^4}\left(\frac{1}{2}-\frac{i\theta}{2\gamma}\right)\Gamma_{q^4}\left(1-\frac{i\theta}{2\gamma}\right)\frac{G_{q^4}^2(1-\frac{i\theta}{2\gamma})}{G_{q^4}^2(\frac{1}{2}-\frac{i\theta}{2\gamma})}, \tag{11}$$

and $\psi_D(\theta) = \vartheta_1^2(\theta|q^2)\psi(\theta)\psi(-\theta)$. The symbol G_q stands for the q-Barnes' G function. The overall constant μ is given by $\vartheta_1'(0|q^2)\psi(0)$.

We stress again that the compact formula (10) is valid for arbitrary ℓ and is free from any approximations. A similar all order formula has been derived for a quantum field theoretical model in Ref. [66] but so far not for lattice models. As an analytic benchmark, we can show that Eq. (10) for $\ell=1$ successfully reproduces [48] the result of the VOA for two spinons [67]. Generally, there is a conjecture [68] about the equivalence of the contributions from 2ℓ spinons and from ℓ particle-hole excitations, which will be analyzed in detail in a separate publication.

Our main result (10) is very efficient for the numerical evaluation of the real-time dynamics. It allows us to obtain $G(m,t)$ for *arbitrary* distances and times, thus going far beyond of what can be achieved by purely numerical algorithms. In Ref. [68] the static correlation functions were investigated within the same framework, but using a Fredholm determinant representation for $\mathcal{A}^{zz}$. This inevitably included a numerical discretization approximation [69]. Although the results seem highly precise, it is important to check them independently as the actual evaluation involves numerical integrations. In the static case, we can establish results with high precision by a relatively small number of sampling points n_p for 2ℓ multiple integrations, see Table I. Once the system starts to evolve in time, however, the numerical difficulty rapidly increases and it becomes necessary to replace the numerical estimation of the Fredholm determinants by an analytic one. To assess the accuracy of a truncated thermal form factor expansion in the dynamic case, we compare results based on the $\ell\le 3$ contributions with data obtained by a

TABLE I. Contributions to the static correlation $G(2,0)$ from small ℓ excitations for $\Delta = 1.1, 1.3$. The last row shows the ratios of the sums of the first three terms in Eq. (5) and the exact values [70], demonstrating that keeping only excitations with $\ell \leq 3$ already leads to highly accurate results.

Δ	1.1	1.3
$I_1(2,0)$	0.2297348	0.2357141
$I_2(2,0)$	3.913377×10^{-2}	6.978269×10^{-3}
$I_3(2,0)$	1.614912×10^{-3}	2.120959×10^{-5}
$(I_1 + I_2 + I_3)/\text{exact}$	0.99951	0.999998

time-dependent density matrix renormalization group algorithm (tDMRG) [71] in Fig. 1. The plots clearly indicate the importance of including not just the $\ell = 1$ but also at least the $\ell = 2$ contribution to obtain results which agree with the tDMRG data on this scale. Based on this comparison, we restrict the following numerics to excitations up to $\ell = 2$ and leave a more detailed discussion of the contributions of higher order excitations for a future study.

There are three asymptotic regimes, characterized by two critical velocities $v_{c_1} < v_{c_2}$ [72], or critical times $t_{c_a} = m/v_{c_a}$ $(a = 1, 2)$. We talk of the space regime if $t < t_{c_2}$, the precursor regime if $t_{c_2} < t < t_{c_1}$, and the time regime if $t > t_{c_1}$. The qualitative differences between the regimes can be better seen for larger m. This is immediately handled by the form factor expansion approach since m enters as a mere parameter. The correlation functions stay largely flat in the space regime, see Fig. 2. Towards the edge of the regime, there occurs an enhancement. After a transient behavior in the precursor regime, the correlation exhibits an oscillatory behavior.

Let us now briefly discuss some technical issues in evaluating Eq. (5). In the time regime, the phase factors can lead to serious numerical instabilities. The ordinary strategy to overcome this problem is to deform the integration contours, making them locally identical to the steepest descendent paths (SDP). This, however, does not work naively in the present case, since the SDPs for particles and holes intersect, which leads to kinematic poles due to $\psi_D(y_j - x_i)$ in the denominator of Eq. (10). To solve this problem, we take advantage of the QTM formulation: we return to finite temperatures and rewrite the formula in such a way that the contribution from the intersecting part is multiplied by the exponentially small factor $e^{-1/T}$. Thus, in the zero temperature limit, one can neglect contributions from the kinematic poles. As a result, the two contours become disentangled and can be treated separately.

Thanks to this trick, stable calculations at long times become possible, see Fig. 3(a). As a further test in the time regime, we compare in Fig. 3(b) our results to those obtained from the two-spinon term in a saddle point approximation [72], which is expected to be valid asymptotically in time. The predicted asymptotic behavior is given by $G(m,t) \sim e^{i\omega t}/t$ for m even with $\omega \sim J$.

Finally, as a first application of Eq. (10), we evaluate the longitudinal DSF $S_{zz}(q,\omega)$, which is directly measurable in neutron scattering experiments. In contrast to S_{+-} [32], the evaluation of S_{zz} in the massive regime is technically difficult and the two-spinon result within the VOA has only recently been reported [73]. On the other hand, Eqs. (5) and (10) allow us to obtain the dynamical correlations for large m and t, and we can readily perform a numerical Fourier transform. We subtract the contribution of the staggered magnetization and include both $\ell = 1$ and $\ell = 2$ excitations. The case $\Delta = 2$ is plotted in Fig. 4 showing that the lineshapes as well as the weights for small q are well resolved. We have checked that the sum rules [74] are satisfied with good accuracy. The $\ell = 1$ excitations are constrained to the spinon energy band with lower and upper boundaries [32] $\omega_{\text{low}} \sim 9.06J$, $\omega_{\text{up}} \sim 11.76J(q = \pi/2)$ and $\omega_{\text{low}} \sim 1.56J$, $\omega_{\text{up}} \sim 16.56J(q = \pi)$, respectively. Higher ℓ excitations lead to a high-frequency tail that becomes more prominent for $\Delta \to 1$ [75]. For larger Δ, the peaks will shift to larger ω and have smaller amplitudes. For $T \ll 1$, the line shape only weakly depends on the magnetic field if it is smaller than the lower critical field, in sharp contrast to the massless case $(|\Delta| < 1)$.

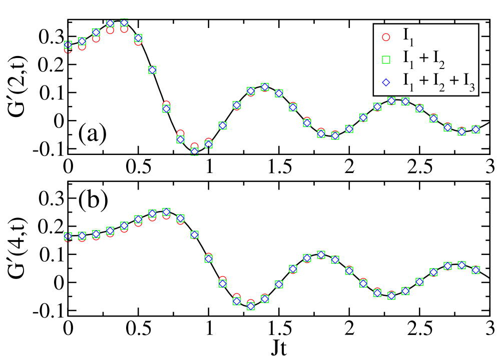

FIG. 1. The real part $G'(m,t) \equiv \Re G(m,t)$ for $\Delta = 1.2$ with (a) $m = 2$, and (b) $m = 4$: Contributions of a thermal form factor expansion (symbols) are compared to tDMRG data (lines).

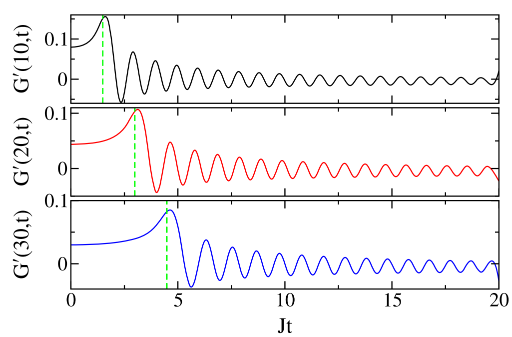

FIG. 2. The real part $G'(m,t)$ for different m and $\Delta = 1.2$. The dashed lines indicate the critical times Jt_{c_1} and Jt_{c_2}. For $\Delta \to 1$, $t_{c_1} \to t_{c_2}$ so there exists only an extremely narrow precursor regime (not visible on this scale) for $\Delta = 1.2$.

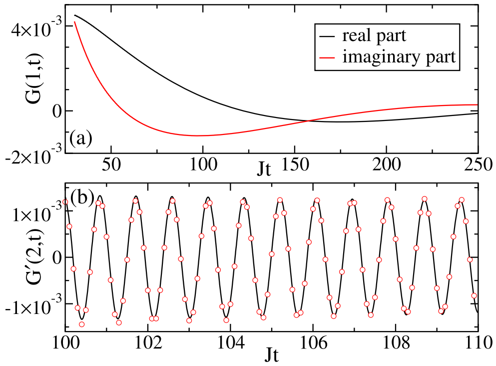

FIG. 3. (a) $G(1,t)$ at long times for $\Delta = 1.2$. (b) Comparison of $G'(2,t)$ obtained by using the form factor expansion (symbols) with the two-spinon asymptotics (line) for $\Delta = 1.4$.

To summarize, we have presented a closed-form expression, incorporating all orders of particle-hole excitations, for the dynamical longitudinal correlation functions of the massive XXZ chain. This result opens up a new avenue to understand the dynamical response of strongly interacting quantum systems and is directly relevant for recent experiments on cold atomic gases. It does also provide a benchmark for the development of numerical algorithms including, for example, recent attempts to learn quantum dynamics using neural networks [76]. We note, furthermore, that the isotropic Heisenberg model, $\Delta = 1$ in Eq. (1), is immediately obtained by rescaling all rapidities x_j, y_j by γx_j, γy_j and by taking $\gamma \to 0$. As all I_ℓ contribute with equal weight to the long-time asymptotic behavior, the explicit formula (10) will be an indispensable tool to study this limit in detail. Extensions to finite temperatures are promising and explicit expressions are already available from thermal form factor expansions if $T/J \ll 1$ [48]. Further progress in dealing with the kinematic poles along the lines of Ref. [60] is expected and will make it possible to access higher temperatures. A detailed analysis of the dynamical structure factor will also be an important subject of future studies.

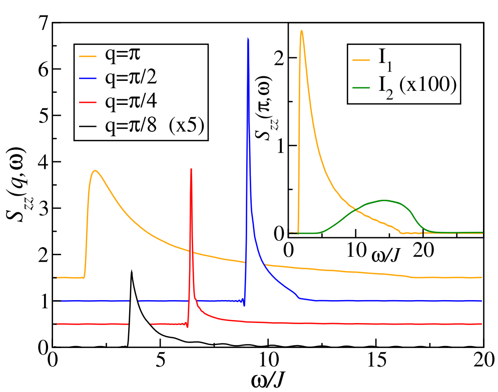

FIG. 4. $S_{zz}(q,\omega)$ with $\Delta = 2$ for various wave numbers q. Note that subsequent curves are shifted vertically by 0.5. Inset: The $\ell = 1$ contribution is nonzero only within the two-spinon continuum $[\omega_{\rm low}, \omega_{\rm up}]$ while $\ell = 2$ excitations contribute also for $\omega > \omega_{\rm up}$.

We thank Andreas Klümper for his continuous encouragement. C. B., F. G., and J. Sirker acknowledge financial support by the German Research Council (DFG) in the framework of the research unit FOR 2316. K. K. K. is supported by CNRS Grant No. PICS07877. J. Sirker acknowledges support by the Natural Sciences and Engineering Research Council (NSERC, Canada). J. Suzuki is supported by JSPS KAKENHI Grants No. 18K03452, No. 18H01141.

[1] B. Paredes, A. Widera, V. Murg, O. Mandel, S. Fölling, I. Cirac, G. V. Shlyapnikov, T. W. Hänsch, and I. Bloch, Tonks-Girardeau gas of ultracold atoms in an optical lattice, Nature (London) **429**, 277 (2004).
[2] S. Hofferberth, I. Lesanovsky, B. Fischer, T. Schumm, and J. Schmiedmayer, Non-equilibrium coherence dynamics in one-dimensional Bose gases, Nature (London) **449**, 324 (2007).
[3] T. Kinoshita, T. Wenger, and D. S. Weiss, A quantum Newton's cradle, Nature (London) **440**, 900 (2006).
[4] M. Gring, M. Kuhnert, T. Langen, T. Kitagawa, B. Rauer, M. Schreitl, I. Mazets, D. A. Smith, E. Demler, and J. Schmiedmayer, Relaxation and prethermalization in an isolated quantum system, Science **337**, 1318 (2012).
[5] V. Guarrera, D. Muth, R. Labouvie, A. Vogler, G. Barontini, M. Fleischhauer, and H. Ott, Spatiotemporal fermionization of strongly interacting one-dimensional bosons, Phys. Rev. A **86**, 021601(R) (2012).
[6] T. Fukuhara, A. Kantian, M. Endres, M. Cheneau, P. Schauß, S. Hild, D. Bellem, U. Schollwöck, T. Giamarchi, C. Gross, I. Bloch, and S. Kuhr, Quantum dynamics of a single, mobile spin impurity, Nat. Phys. **9**, 235 (2013).
[7] T. Fukuhara, P. Schauss, M. Endres, S. Hild, M. Cheneau, I. Bloch, and C. Gross, Microscopic observation of magnon bound states and their dynamics, Nature (London) **502**, 76 (2013).
[8] S. Hild, T. Fukuhara, P. Schauß, J. Zeiher, M. Knap, E. Demler, I. Bloch, and C. Gross, Far-From-Equilibrium Spin Transport in Heisenberg Quantum Magnets, Phys. Rev. Lett. **113**, 147205 (2014).
[9] P. N. Jepsen, J. Amato-Grill, I. Dimitrova, W. W. Ho, E. Demler, and W. Ketterle, Spin transport in a tunable Heisenberg model realized with ultracold atoms, Nature (London) **588**, 403 (2020).
[10] N. Motoyama, H. Eisaki, and S. Uchida, Magnetic Susceptibility of Ideal Spin 1/2 Heisenberg Antiferromagnetic Chain Systems, Sr_2CuO_3 and $SrCuO_2$, Phys. Rev. Lett. **76**, 3212 (1996).
[11] M. Takigawa, N. Motoyama, H. Eisaki, and S. Uchida, Field-induced staggered magnetization near impurities in the $s = 1/2$ one-dimensional Heisenberg antiferromagnet Sr_2CuO_3, Phys. Rev. B **55**, 14129 (1997).
[12] K. R. Thurber, A. W. Hunt, T. Imai, and F. C. Chou, ^{17}O NMR study of $q = 0$ Spin Excitations in a Nearly Ideal

$S = 1/2$ 1D Heisenberg Antiferromagnet, Sr_2CuO_3, up to 800 K, Phys. Rev. Lett. **87**, 247202 (2001).
[13] M. Mourigal, M. Enderle, A. Klöpperpieper, J.-S. Caux, A. Stunault, and H. M. Ronnow, Fractional spinon excitations in the quantum Heisenberg antiferromagnetic chain, Nat. Phys. **9**, 435 (2013).
[14] A. V. Sologubenko, K. Giannó, H. R. Ott, A. Vietkine, and A. Revcolevschi, Heat transport by lattice and spin excitations in the spin-chain compounds $SrCuO_2$ and Sr_2CuO_3, Phys. Rev. B **64**, 054412 (2001).
[15] A. V. Sologubenko, K. Berggold, T. Lorenz, A. Rosch, E. Shimshoni, M. D. Phillips, and M. M. Turnbull, Magnetothermal Transport in the Spin-$\frac{1}{2}$ Chains of Copper Pyrazine Dinitrate, Phys. Rev. Lett. **98**, 107201 (2007).
[16] N. Hlubek, P. Ribeiro, R. Saint-Martin, A. Revcolevschi, G. Roth, G. Behr, B. Büchner, and C. Hess, Ballistic heat transport of quantum spin excitations as seen in $SrCuO_2$, Phys. Rev. B **81**, 020405(R) (2010).
[17] Y. Kohama, A. V. Sologubenko, N. R. Dilley, V. S. Zapf, M. Jaime, J. A. Mydosh, A. Paduan-Filho, K. A. Al-Hassanieh, P. Sengupta, S. Gangadharaiah, A. L. Chernyshev, and C. D. Batista, Thermal Transport and Strong Mass Renormalization in $NiCl_2$-$4SC(NH_2)_2$, Phys. Rev. Lett. **106**, 037203 (2011).
[18] A. Imambekov and L. I. Glazman, Universal theory of nonlinear Luttinger liquids, Science **323**, 228 (2009).
[19] A. Imambekov, T. L. Schmidt, and L. I. Glazman, One-dimensional quantum liquids: Beyond the Luttinger liquid paradigm, Rev. Mod. Phys. **84**, 1253 (2012).
[20] R. G. Pereira, S. R. White, and I. Affleck, Exact Edge Singularities and Dynamical Correlations in Spin-1/2 Chains, Phys. Rev. Lett. **100**, 027206 (2008).
[21] R. G. Pereira, Long time correlations of nonlinear Luttinger liquids, Int. J. Mod. Phys. B **26**, 1244008 (2012).
[22] J. Sirker, The Luttinger liquid and integrable models, Int. J. Mod. Phys. B **26**, 1244009 (2012).
[23] O. A. Castro-Alvaredo, B. Doyon, and T. Yoshimura, Emergent Hydrodynamics in Integrable Quantum Systems Out of Equilibrium, Phys. Rev. X **6**, 041065 (2016).
[24] A. Urichuk, Y. Oez, A. Klümper, and J. Sirker, The spin drude weight of the XXZ chain and generalized hydrodynamics, SciPost Phys. **6**, 005 (2019).
[25] V. B. Bulchandani, R. Vasseur, C. Karrasch, and J. E. Moore, Bethe-Boltzmann hydrodynamics and spin transport in the XXZ chain, Phys. Rev. B **97**, 045407 (2018).
[26] B. Bertini, M. Collura, J. De Nardis, and M. Fagotti, Transport in Out-of-Equilibrium XXZ Chains: Exact Profiles of Charges and Currents, Phys. Rev. Lett. **117**, 207201 (2016).
[27] J. D. Nardis, D. Bernard, and B. Doyon, Diffusion in generalized hydrodynamics and quasiparticle scattering, SciPost Phys. **6**, 49 (2019).
[28] E. H. Lieb, T. Schultz, and D. Mattis, Two soluble models of an antiferromagnetic chain, Ann. Phys. (N.Y.) **16**, 407 (1961).
[29] T. T. Wu, B. M. McCoy, C. A. Tracy, and E. Barouch, Spin-spin correlation functions for 2-dimensional Ising model—exact theory in scaling region, Phys. Rev. B **13**, 316 (1976).
[30] T. Niemeijer, Some exact calculations on a chain of spins $\frac{1}{2}$, Physica **36**, 377 (1967).
[31] M. Jimbo, K. Miki, T. Miwa, and A. Nakayashiki, Correlation functions of the XXZ model for $\Delta < -1$, Phys. Lett. A **168**, 256 (1992).
[32] A. H. Bougourzi, M. Karbach, and G. Müller, Exact two-spinon dynamic structure factor of the one-dimensional $s = 1/2$ Heisenberg-Ising antiferromagnet, Phys. Rev. B **57**, 11429 (1998).
[33] A. Abada, A. H. Bougourzi, and B. Si-Lakhal, Exact four-spinon dynamical correlation function of the Heisenberg model, Nucl. Phys. **B497**, 733 (1997).
[34] J.-S. Caux, J. Mossel, and I. P. Castillo, The two-spinon transverse structure factor of the gapped Heisenberg antiferromagnetic chain, J. Stat. Mech. (2008) P08006.
[35] J.-S. Caux and R. Hagemans, The 4-spinon dynamical structure factor of the Heisenberg chain, J. Stat. Mech. (2006) P12013.
[36] H. Boos, M. Jimbo, T. Miwa, F. Smirnov, and Y. Takeyama, Hidden Grassmann structure in the XXZ model II: Creation operators, Commun. Math. Phys. **286**, 875 (2009).
[37] M. Jimbo, T. Miwa, and F. Smirnov, Hidden Grassmann structure in the XXZ model III: Introducing Matsubara direction, J. Phys. A **42**, 304018 (2009).
[38] J. Sato, B. Aufgebauer, H. Boos, F. Göhmann, A. Klümper, M. Takahashi, and C. Trippe, Computation of Static Heisenberg-Chain Correlators: Control Over Length and Temperature Dependence, Phys. Rev. Lett. **106**, 257201 (2011).
[39] T. Miwa and F. Smirnov, New exact results on density matrix for XXX spin chain, Lett. Math. Phys. **109**, 675 (2019).
[40] V. E. Korepin, N. M. Bogoliubov, and A. G. Izergin, *Quantum Inverse Scattering Method and Correlation Functions* (Cambridge University Press, Cambridge, England, 1993).
[41] N. Kitanine, J. M. Maillet, and V. Terras, Form factors of the XXZ Heisenberg spin-$\frac{1}{2}$ finite chain, Nucl. Phys. **B554**, 647 (1999).
[42] N. A. Slavnov, Calculation of scalar products of the wave functions and form factors in the framework of the algebraic Bethe ansatz, Teor. Mat. Fiz. **79**, 232 (1989).
[43] N. Kitanine, K. K. Kozlowski, J. M. Maillet, N. A. Slavnov, and V. Terras, A form factor approach to the asymptotic behavior of correlation functions in critical models, J. Stat. Mech. (2011) P12010.
[44] N. Kitanine, K. K. Kozlowski, J. M. Maillet, N. A. Slavnov, and V. Terras, Form factor approach to dynamical correlation functions in critical models, J. Stat. Mech. (2012) P09001.
[45] J. L. Cardy, Operator content of two-dimensional conformally invariant theories, Nucl. Phys. **B270**, 186 (1986).
[46] J.-S. Caux and J. M. Maillet, Computation of Dynamical Correlation Functions of Heisenberg Chains in a Field, Phys. Rev. Lett. **95**, 077201 (2005).
[47] F. Göhmann, M. Karbach, A. Klümper, K. K. Kozlowski, and J. Suzuki, Thermal form-factor approach to dynamical correlation functions of integrable lattice models, J. Stat. Mech. (2017) 113106.
[48] C. Babenko, F. Göhmann, K. K. Kozlowski, and J. Suzuki, A thermal form factor series for the longitudinal two-point function of the Heisenberg-Ising chain in the antiferromagnetic massive regime, J. Math. Phys. (N.Y.) **62**, 041901 (2021).

[49] https://dlmf.nist.gov.

[50] See Supplemental Material at http://link.aps.org/supplemental/10.1103/PhysRevLett.126.210602 for some background material and a derivation of Eq. (10), which includes Refs. [51–53].

[51] E. T. Whittaker and G. N. Watson, in *A Course of Modern Analysis*, 4th ed. (Cambridge University Press, Cambridge, England, 1963), Chap. 21.

[52] M. Dugave, F. Göhmann, and K. K. Kozlowski, Thermal form factors of the XXZ chain and the large-distance asymptotics of its temperature dependent correlation functions, J. Stat. Mech. (2013) P07010.

[53] N. Kitanine and G. Kulkarni, Thermodynamic limit of the two-spinon form factors for the zero field XXX chain, SciPost Phys. **6**, 076 (2019).

[54] M. Suzuki, Transfer-matrix method and Monte Carlo simulation in quantum spin systems, Phys. Rev. B **31**, 2957 (1985).

[55] J. Suzuki, Y. Akutsu, and M. Wadati, A new approach to quantum spin chains at finite temperature, J. Phys. Soc. Jpn. **59**, 2667 (1990).

[56] A. Klümper, Free energy and correlation length of quantum chains related to restricted solid-on-solid lattice models, Ann. Phys. (Leipzig) **1**, 540 (1992).

[57] F. Göhmann, A. Klümper, and A. Seel, Integral representations for correlation functions of the XXZ chain at finite temperature, J. Phys. A **37**, 7625 (2004).

[58] H. Boos, F. Göhmann, A. Klümper, and J. Suzuki, Factorization of the finite temperature correlation functions of the XXZ chain in a magnetic field, J. Phys. A **40**, 10699 (2007).

[59] K. Sakai, Dynamical correlation functions of the XXZ model at finite temperature, J. Phys. A **40**, 7523 (2007).

[60] F. Göhmann, K. K. Kozlowski, J. Sirker, and J. Suzuki, Equilibrium dynamics of the XX chain, Phys. Rev. B **100**, 155428 (2019).

[61] O. Babelon, H. J. de Vega, and C. M. Viallet, Analysis of the Bethe Ansatz equations of the XXZ model, Nucl. Phys. **B220**, 13 (1983).

[62] A. Virosztek and F. Woynarovich, Degenerated ground states and excited states of the $S = \frac{1}{2}$ anisotropic antiferromagnetic Heisenberg chain in the easy axis region, J. Phys. A **17**, 3029 (1984).

[63] M. Takahashi, *Thermodynamics of One-Dimensional Solvable Models* (Cambridge University Press, Cambridge, England, 1999).

[64] M. Dugave, F. Göhmann, K. K. Kozlowski, and J. Suzuki, Low-temperature spectrum of correlation lengths of the XXZ chain in the antiferromagnetic massive regime, J. Phys. A **48**, 334001 (2015).

[65] G. Gasper and M. Rahman, *Basic Hypergeometric Series* (Cambridge University Press, Cambridge, England, 2004).

[66] F. A. Smirnov, A general formula for soliton form factors in the quantum sine-Gordon model, J. Phys. A **19**, L575 (1986).

[67] M. Lashkevich, Free field construction for the eight-vertex model: representation for form factors, Nucl. Phys. **B621**, 587 (2002).

[68] M. Dugave, F. Göhmann, K. K. Kozlowski, and J. Suzuki, Thermal form factor approach to the ground-state correlation functions of the XXZ chain in the antiferromagnetic massive regime, J. Phys. A **49**, 394001 (2016).

[69] F. Bornemann, On the numerical evaluation of Fredholm determinants, Math. Comput. **79**, 871 (2010).

[70] M. Takahashi, G. Kato, and M. Shiroishi, Next nearest-neighbor correlation functions of the spin-$1/2$ XXZ chain at massive region, J. Phys. Soc. Jpn. **73**, 245 (2004).

[71] T. Enss and J. Sirker, Lightcone renormalization and quantum quenches in one-dimensional Hubbard models, New J. Phys. **14**, 023008 (2012).

[72] M. Dugave, F. Göhmann, K. K. Kozlowski, and J. Suzuki, Asymptotics of correlation functions of the Heisenberg-Ising chain in the easy-axis regime, J. Phys. A **49**, 07LT01 (2016).

[73] I. P. Castillo, The exact two-spinon longitudinal dynamical structure factor of the anisotropic XXZ model, arXiv:2005.10729.

[74] G. Müller, Sum rules in the dynamics of quantum spin chains, Phys. Rev. B **26**, 1311 (1982).

[75] R. Pereira, J. Sirker, J.-S. Caux, R. Hagemans, J. M. Maillet, S. R. White, and I. Affleck, Dynamical structure factor at small q for the XXZ spin-$1/2$ chain, J. Stat. Mech. (2007) P08022.

[76] G. Carleo and M. Troyer, Solving the quantum many-body problem with artificial neural networks, Science **355**, 602 (2017).